Article:
White, AL, Langton, C, Wille, ML et al. (7 more authors) (2019) Ultrasound-triggered release from metal shell microcapsules. Journal of Colloid and Interface Science, 554. pp. 444-452. ISSN 0021-9797

https://doi.org/10.1016/j.jcis.2019.07.020

Ultrasound-Triggered Release from Metal Shell Microcapsules

Alison L. White[1,2,3]*, Christian Langton[4], Marie-Luise Wille[4], James Hitchcock[5], Olivier J. Cayre[5], Simon Biggs[6], Idriss Blakey,[1,7] Andrew K. Whittaker[1,3], Stephen Rose[2], Simon Puttick[2]

1. Australian Institute of Bioengineering and Nanotechnology, The University of Queensland, St. Lucia, Queensland, 4072, Australia.
2. CSIRO Probing Biosystems Future Science Platform, Brisbane, Australia
3. ARC Centre of Excellence in Convergent Bio-Nano Science and Technology, The University of Queensland, St Lucia, 4072, Australia
4. Institute of Health Biomedical Innovation, Queensland University of Technology, Kelvin Grove, 4059, Australia
5. School of Chemical and Process Engineering, University of Leeds, Leeds, LS2 9JT, UK
6. The University of Western Australia, Perth, Western Australia, 6009, Australia.
7. Centre for Advanced Imaging, The University of Queensland, St. Lucia, Queensland, 4072, Australia.

*a.tasker@uq.edu.au

Encapsulation, triggered release, focused ultrasound, metal microcapsules, delivery vehicle

Abstract

Metal shell microcapsules have been shown to completely retain their core until its release is triggered, making them a promising candidate for use as a controllable drug delivery vehicle due to their superior retention properties as compared to polymer shell microcapsules. Focused ultrasound (FUS) has been successfully utilised to trigger release of lipophilic drugs from polymer microcapsules, and in this work the response of gold shell microcapsules with and without an inner polymeric shell, to FUS and standard ultrasound is explored. The results show that gold shell microcapsules with an inner polymer shell rupture when exposed to standard ultrasound and that there is a linear correlation between the gold shell thickness and the extent of shell rupture. When FUS is applied to these microcapsules, powers as low as 0.16 W delivered in bursts of 10 ms/s over a period of 120 s are sufficient to cause rupture of 53 nm gold shell microcapsules. Additional findings suggest that gold shell microcapsules without the polymer layer dispersed in a hydrogel matrix, as opposed to aqueous media, rupture more efficiently when exposed to FUS, and that thicker gold shells are more responsive to ultrasound-triggered rupture regardless of the external environment. Release of dye from all successfully ruptured capsules was sustained over a period of between 7-35 days. These findings suggest that emulsion-templated gold shell microcapsules embedded in a hydrogel matrix would be suitable for use as an implantable drug delivery vehicle with FUS used to externally trigger release.

Introduction

Encapsulation is a method frequently employed across a vast range of industries,[1-7] to provide protection and the ability to control release of active ingredients. Typically, polymers have been the shell material of choice, with a range of methods, such as solvent evaporation, coacervation, interfacial polymerisation, and layer-by-layer deposition,[8-11] available for synthesis of such microcapsules. In addition, starting materials are readily available, making polymer materials a standard choice for encapsulation. However, due to the inherent porosity of polymer films/shells, complete retention of small molecular weight active ingredients is inefficient and much work in the literature has focused on improving the retention properties of polymer microcapsules, for example by cross-linking, or increasing the polymer shell thickness.[10, 12] Unfortunately, these improvements only retard diffusion of small molecules across the polymer membrane by a few hours to weeks, thus by no means offering complete retention.

More recently metal-shell polymer microcapsules have been a new focus in encapsulation research owing to the impermeable nature of the metal film and thus superior barrier properties when compared to polymer shells alone.[13-18] Our previous work showed that when gold shells of 70 nm are grown using electroless deposition onto poly(methyl methacrylate) (PMMA) microcapsules, the core material is fully retained for at least 21 days at 40°C in an environment that can dissolve the microcapsule core.[13] The unique property of metal shells to render the microcapsules impermeable allows for advances to be made in the field of encapsulation for drug delivery, particularly for actives where premature release can cause serious off-target side effects, such as anti-cancer drugs. To successfully utilise the advantages provided by such metal shells however, one must be able to trigger release of the actives at the desired time and location within the body, for example at the site of a tumour.

Separately, there is much work in the literature, which uses ultrasound waves to trigger release from polymer microcapsules.[19-23] For example, Lensen et al. prepared perfluorooctanol-poly(lactic acid) microcapsules with different initial polymer concentrations to achieve a series of polymer capsule samples with different shell thicknesses.[21] They applied an ultrasonic pressure pulse to the capsules and found that pressures above 250 kPa were required before any deformation was seen, even on the thinnest polymer shells. Wang et al. demonstrated that by applying pulsed ultrasound at a power of 9 W to alginate capsules containing diclofenac, they were able to increase the rate of drug release.[22] The presence of metal nanoparticles has also been shown to enhance the effects of ultrasound on capsule rupture due to the acoustic waves being enhanced as they pass through media of different densities.[24] Skirtach et al. showed that by embedding silver nanoparticles into PSS/PAH polymer microcapsules, they were able to augment the sensitivity of the capsules to the effects of acoustic waves, by increasing the bulk density of the shell.[25] Kijewska et al. also demonstrated that the incorporation of gold nanoparticles into polymer capsule shells can enhance the effects of ultrasound.[26] They encapsulated an aqueous suspension of gold nanoparticles in polypyrrole microcapsules, and upon sonication for 1 minute at 9.3 W found that the capsules were completely fractured. On the contrary polymer capsules in the absence of gold nanoparticles remained intact.

In this work, we examine the efficacy of ultrasound as a tool for triggering release of small molecules from metal-shell microcapsules and develop an increased understanding of the factors that affect capsule breakage. Whilst there are large bodies of work on ultrasonic breakage of polymer capsules and metal nanoparticle modified polymer capsules, as far as the authors know, only a few studies use ultrasound as a tool to break metal shells. Sun et al. sonicated silver-coated colloidosomes at 20 kHz, fracturing the capsules to trigger release of a dye into solution, with approximately 10% release after 425 hours. However, upon application of high intensity focused ultrasound at 2.65 MHz frequency and 6 W, they observed only some of the silver shells showing mechanical damage.[18] In addition, within our group we have recently presented that large, 20-50 μm gold coated emulsion droplets can be fractured using focused ultrasound, although release of the core is not quantified. Here we present quantification of ultrasound-triggered rupture of smaller gold shell microcapsules, using fluorescence spectroscopy to monitor dye release in two different bulk environments, aqueous suspension and hydrogel matrix. We investigate the effect of exposure time and power of the ultrasound signal on the breakage of a range of metal coated microcapsules including the elimination of the polymer layer by using metal coated emulsions, at clinically relevant ultrasound frequencies and pressures using both non-focused ultrasound (US) and focused ultrasound (FUS).

Materials and methods

2.1 Materials

Poly(lactic-co-glycolic acid), (PLGA), (50:50) (10-15 kDa), dichloromethane, (DCM); poly(vinyl pyrollidone) (PVP) (40KDa); chloroplatinic acid 99%, (H_2PtCl_6); chloroauric acid 99.99% ($HAuCl_4$); perfluorooctyl bromide(PFOB); 30% hydrogen peroxide, (H_2O_2); and sodium borohydride ($NaBH_4$) 98%; d,l-lactide; glycolide; tin octoate ($Sn(oct)_2$); 2-[(1E,3E)-3-(3,3-Dimethyl-1-octadecyl-1,3-dihydro-2H-indol-2-ylidene)-1-propen-1-yl]-3,3-dimethyl-1-octadecyl-3H-indolium perchlorate (DiI) and poly(ethylene glycol) (PEG) (1000 Da) were purchased from Sigma. Miglyol 812 was provided as a gift from IOI Oleo GmbH. ^{3}H Paclitaxel (20 Ci/mmol) was purchased from ViTrax, USA. All chemicals were used as received.

2.2.1 Gold shell deposition onto PLGA microcapsules with embedded Pt nanoparticles.

PLGA microcapsules with embedded PVP-Pt nanoparticles were synthesised as described previously.[17] A H_2PtCl_6 concentration of 2.2 mM was used to prepare the PVP-Pt nanoparticles used to stabilise the PLGA microcapsules. The microcapsules were dispersed in 25 mL ultrapure water. 0.5 mL of microcapsule dispersion was added to a gold plating solution of $HAuCl_4$ (1.0 ml, 40 mM), PVP (3.0 ml, 0.05 mM) and H_2O_2 (1.0 ml, 60 mM) and mixed on a vertical rotator for 5 minutes at 50 rpm. The capsules were washed via centrifugation at 2000 rpm for 2 minutes at room temperature, three times and redispersed in 3 ml Milli-Q water with 0.2 ml PVP (0.05 mM) as a stabiliser to prevent aggregation. To investigate the effect of metal shell thickness on resistance to ultrasound ablation the $HAuCl_4$ concentration was reduced to 20 mM, 10 mM, 5 mM and 2 mM.

2.2.2 Gold shell deposition onto PVP-Pt stabilised emulsion droplets.

First, PVP-Pt nanoparticles were synthesised using a modified method to that described previously, whereby 0.23 g H_2PtCl_6 was dissolved in 100 mL PVP solution (0.00625 wt%), then reduced by rapid injection of 2 mL

$NaBH_4$ (1.1 M). After 24 hours the resulting nanoparticles were filtered using a 0.2 µm syringe filter, and used within 3 months. 1 mL of PVP-Pt nanoparticles was added to an Eppendorf tube containing either 0.1 mL of miglyol 812, 0.095 mL miglyol and 0.005 mL DiI (10 ug.mL^{-1} in ethanol), or 0.07 mL miglyol and 0.03 mL ^{3}H paclitaxel, and the sample was emulsified using a Branson Sonifier 450 Ultrasonic Homogeniser (Consonic, Australia) for 45 s four times, resting in ice for at least –60 s between sonication bursts. The resulting PVP-Pt stabilised emulsion was allowed to cream overnight and excess nanoparticles in the aqueous phase were removed and the emulsion was redispersed in 1 mL Ultrapure water. 0.25 mL of the redispersed emulsion was added to a gold plating solution of $HAuCl_4$ (0.75 ml or 2 mL, 40 mM), PVP (0.5 ml, 0.05 mM) and H_2O_2 (0.75 mL or 2 mL, 60 mM) and Milli-Q water to give a total volume of 11.75 mL. The dispersion was mixed on a vertical rotator for 5 minutes at 50 rpm and the resulting microcapsules were washed via centrifugation at 2000 rpm for 2 minutes at room temperature, three times and redispersed in 3 ml Milli-Q water.

2.2.3 Synthesis of poly(lactide-co-glycolide)-poly(ethylene glycol)-poly(lactide-co-glycolide) (PLGA-PEG-PLGA)

PLGA-PEG-PLGA was formed by ring-opening polymerisation.[27] Briefly, Poly(ethylene glycol) PEG 1000 (5.99g) was dried under vacuum for 2.5 hours at 110 ℃ in a round bottomed flask. After cooling to room temperature, d,l-lactide (11.01 g) and glycolide (2.99 g) were added and heated to melt, under an argon atmosphere. Tin 2-ethylhexanoate (3.25 µL) was added and the mixture was heated to 130 ℃ for 18 hours. The crude product was dissolved in ice cold water before heating to 80 ℃ to precipitate the polymer. The aqueous phase was removed and this process was repeated twice. The purified polymer was lyophilised to give a final yield of 55%. Gel permeation chromatography (GPC) was used to determine molecular weight and polydispersity, using dimethylacetamide with 0.3 wt% lithium chloride as the solvent. ^{1}H NMR was used to confirm the synthesis of the polymer.

To prepare the thermo-setting hydrogel a 15 wt% solution of the PLGA-PEG-PLGA polymer was prepared in Milli-Q water at 4 ℃. The gelation point of the hydrogel was 16 ℃, below which gelation did not occur.

2.2.4 Triggered release using ultrasound

2 mL of gold-coated polymer microcapsules of desired shell thickness was added to a tube with an SEM stub secured in an upright position at the bottom of the tube (Figure S2a). A 0.5” single element, unfocused 1 MHz broadband transducer (Olympus, Waltham, MA, USA) was placed in the tube, submersed in the sample. A second, identical transducer was used to test reproducibility. A thermocouple was inserted down the side of the transducer, outside of the path of the ultrasound signal to monitor temperature changes throughout the experiments. A radio-frequency power amplifier (Electronics & Innovation, Rochester, NY, USA) was used to amplify the power applied to the sample from a 50 MHz arbitrary generator (Hameg HMF2525, now Rohde&Schwarz, Munich, Germany). The generated signal was monitored using an oscilloscope (Agilent). For the initial experiments the power applied to the sample was set at 41 W ± 2 W and was applied as a continuous wave to each of the four samples of varying metal shell thickness for 10 minutes. Each test was repeated in triplicate. In separate experiments the exposure time was reduced to 5 minutes and 2 minutes, and the power

was reduced to 18 W ± 1 W and 9 W ± 1 W. In all cases the ultrasonic frequency was set to the transducer resonance frequency at 965 kHz, which was determined experimentally.

Two identical ultrasound transducers were used in this work to assess reproducibility, as the first transducer became inefficient due to overheating. The number of capsules ruptured was calculated by counting all the visible capsules from a collection of SEM images and assessing which of these were ruptured or still intact. During the experiment the bulk temperature was monitored using a thermocouple. Across the studies temperature increases of between 3 and 30 °C were measured, dependent on exposure time and ultrasound power. Capsules with holes similar to those seen when heat alone (Figure S2) was applied to the capsule sample were taken to be intact, as this damage was deemed not to be from the ultrasound. Agglomerated capsules were discounted in this analysis in instances where discreet capsules could not be resolved.

2.2.5 Triggered release using focused ultrasound

As a comparison to the standard ultrasound results, gold-coated polymer microcapsules were subjected to focused ultrasound using an LP-100 Focused Ultrasound (FUS) system (FUS Instruments, Canada). The FUS set-up can be seen in Figure S1a). Ultrapure water was degassed using a SRDS-1000 water degassing system (FUS Instruments, Canada) for at least 2 hours prior to filling the ultrasound chambers. A 1.1 MHz conical transducer with hydrophone was used to emit the ultrasound waves. The focal point was set at a position of L 0 mm, I 0 mm and A 10 mm, corresponding to the transducers x-, y- and z-coordinates respectively. When the fountain was just visible at the meniscus, the focus was in the correct position. A plastic tube of 10 mm internal diameter was used as the sample holder and threaded through holes on either side of the water chamber to immerse it at the set focal point and immobilise it. The water chamber was then filled to the top and 0.5 mL of sample was injected into the tube to completely fill it from end to end to ensure no air bubbles were present. Prior to sonication a foam cover was placed over the chamber to absorb the ultrasound. Two gold shell thicknesses were investigated, 53 and 80 nm and were exposed to 10 ms bursts every 1 s for a period of 120 s at acoustic pressures of 5 MPa, 2.5 MPa and 0.5 MPa, corresponding to powers of 14 W, 3.7 W and 0.16 W respectively.

For the gold-shelled emulsions, the effect of changing the dispersion media, aqueous solution or hydrogel matrix was investigated for two different shell thicknesses, 80 nm and 250 nm. A sample holder was built in-house to hold 8 x 1 cm^3 samples. 0.1 mL of microcapsules was added to either 0.9 mL of Ultrapure water or 0.9 mL of PLGA-PEG-PLGA solution (15 wt%) at 4 °C. The hydrogel was allowed to phase change from a sol to a gel and the samples were degassed in a vacuum oven at room temperature for 30 min prior to sonication. Focus finding was guided using an MRI image of the sample holder loaded into the FUS control software and the focus for each sample was targeted using the software, Figure S1b. The ultrasound conditions used were as above.

2.2.6 Characterisation of metal microcapsules

Size distribution of the microcapsules was measured using a Malvern Mastersizer and the size distribution of the gold-shelled emulsions was measured from optical microscopy images using image analysis software,

ImageJ.[28] The metal shell thickness was measured and analysed using serial block face imaging of the microcapsules or gold-coated emulsions embedded in an epoxy resin, (Zeiss Sigma Scanning Electron Microscope with Gatan 3View), and analysed using Matlab as described previously.[17] For those gold-coated emulsion samples which collapsed upon drying, atomic force microscopy (Cypher AFM) was used to measure the height profile of broken fragments of shell, dried onto silicon wafers and cleaned with ethanol to remove oil residues, to find the shell thickness. To account for both walls of the collapsed capsule, the recorded height was halved before being reported. Scanning electron microscopy (Hitachi SU3500) under low vacuum, and cryo-scanning electron microscopy (JEOL JSM-7100F with GATAN Alto2500 cryo-preparation system) were used to observe the structure of gold coated emulsions.

To assess the resulting capsule morphology (intact or broken) after ultrasound treatment, the sample collected on the SEM stub was imaged using a Hitachi SU3500 scanning electron microscope. Images were analysed using ImageJ to count the proportion of broken capsules as compared to intact capsules. To quantify release of DiI from gold-coated emulsion droplets after ultrasound exposure, 1 mL absolute ethanol was added to the samples and 180 µL was added to a 96 well plate for fluorescence intensity measurements, with 540 nm excitation and 570 nm emission wavelengths used, on an Infinite 200Pro Microplate reader (Tecan). The concentration of DiI released was calculated from a concentration vs absorbance standard curve of DiI in 50:50 ethanol:water.

Results and discussion

3.1 Synthesis of metal shell microcapsules and emulsions for ultrasound triggered release

In this work, the ability to remotely trigger release by breaking gold shell microcapsules was explored. We chose initially to explore gold coated polymer microcapsules as used in our previous work, containing an ultrasound contrast agent, perfluorooctyl bromide (PFOB) as the model core.[17] Polymer microcapsules containing PFOB were synthesised using the solvent evaporation method to give microcapsules of 2-7 µm diameter, with platinum nanoparticles embedded at the surface. For the electroless deposition of the continuous gold shell, gold salt concentration was varied as described in our previous work, to give a shell thicknesses of between 43 and 80 nm, as seen in Figure 1a.

The second microcapsule system we explored was a gold coated emulsion droplet, as first described in our recent work.[29] By removing the polymer shell and depositing a continuous gold shell directly onto the stabilised oil droplet, the encapsulation efficiency can be increased dramatically, as the shell thickness to radius ratio can be reduced to almost 1 %. The nanoparticle-stabilised emulsion template was prepared by sonication and this allowed for a more uniform size distribution of droplets to be formed as compared to the polymer microcapsules, with a mean diameter of 12.5 ± 2.8 µm. The platinum nanoparticles, which stabilised the oil droplet templates were used to localise and catalyse the deposition of a continuous gold shell at the interface, as described in our previous work.[17] Miglyol 812 was used as the core oil for the gold coated emulsions as it is an FDA approved carrier oil for pharmaceuticals, and, unlike PFOB, was able to dissolve the fluorescent dye, DiI, required for assessing release from ruptured capsules following exposure to ultrasound. Careful choice of

fluorescent dye was required for the release study as many common dyes were found to either inhibit the gold shell formation, or adsorbed to the gold layer and thus could not be released upon rupture of the shells.

3.2 Determination of ultrasound as a suitable trigger for microcapsule rupture

Initially unfocused ultrasound was applied to the samples as a proof of concept. A 1 MHz transducer was used as this frequency is within a clinically feasible range, and this was connected to a power amplifier, which allowed powers of up to 40 W to be generated. In these initial experiments, the ultrasound power, exposure time and capsule shell thickness were investigated.

It was anticipated, based on recent modelling studies performed in the literature[30] and subsequent experimental observations, that capsules with a thinner shell would break more readily than those with thicker shells. This anticipated phenomenon is believed to be due to capsules with a higher shell to diameter ratio being able to better withstand expansion of the core material in response to the ultrasound.[21] Cavitation occurs when acoustic signals cause microbubbles to form on the basis of the air dissolved in the capsule dispersion continuous phase. These microbubbles oscillate due to the shear created by the ultrasonic wave and eventually collapse, resulting in a large energy release. This microbubble collapse leads to shear forces, which disrupt the capsule membrane, causing it to rupture.[24] Microcapsule gold shells have a reduced elasticity as compared to that of polymer shells, thus making them more susceptible to rupture under these conditions.[31] Indeed, the results in Figure 1 show a linear trend between the proportion of capsules that ruptured upon ultrasound exposure and the shell thickness.

The thinnest shells (~40 nm) responded most effectively to ultrasound exposure with 95 - 100% of the capsules rupturing after 10 minutes at 41 W continuous wave ultrasound. Whilst the proportion of burst capsules varied with different transducers, the influence of capsule shell thickness remained the same, with the exception of the 43 ±14 nm shells which showed a smaller, but maximum possible increase in breakage from 95% to 100% when the second transducer was used. Figure 1b shows an SEM micrograph of microcapsules with a 53 ±10 nm gold shell having ruptured after exposure to the 41 ± 2 W continuous wave ultrasound for 10 minutes.

Finally, the ultrasound power required to rupture the microcapsules was considered. The scanning electron micrograph presented Figure 1c shows that reducing the ultrasound power from 41 ± 2 W down to 9 ± 1 W, with an exposure time of 2 minutes, does not affect its ability to cause capsule rupture, which is consistent with other studies that have used ultrasound to burst metal nanoparticle-embedded polymer microcapsules.[25-26] This suggests that the ultrasound waves cause a damaging effect in short time periods, when bulk heating is less than 5 ℃and confirms that the rupture is due to cavitation caused by the ultrasonic waves on the capsules as opposed to an overall heating effect.[22] It is important to note that the capsules that remained intact after application of the ultrasound were at the lower end of the size distribution range in all cases, below approximately 2 µm in diameter. This is likely due to the increased structural integrity of smaller spheres as a result of their larger shell thickness-to-diameter ratio. Indeed, Kolesnikova et al. found that polymer microcapsules prepared by layer-by-layer deposition onto 5.3 µm particle templates required longer exposure to ultrasound for breakage to occur compared to the same polymer deposition on 9.6 µm templates.[32]

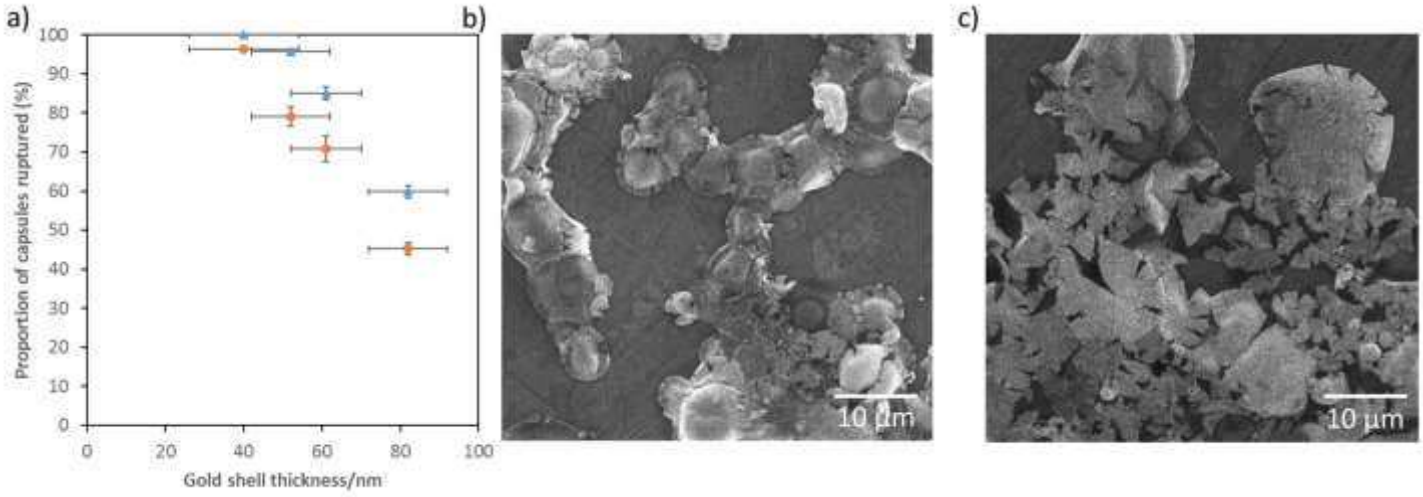

Figure 1 – a) Effect of metal shell thickness on the proportion of capsules ruptured when subjected to 965 kHz ultrasound at 41 ± 2 W for 10 minutes, for two identical transducers. (Shell thickness determined from serial block face analysis as described previously).[17] Scanning electron micrographs showing b) ruptured capsules with a shell thickness of 53 ± 10 nm at 41 ± 2 W with 10 minute continuous exposure, and c) ruptured capsules with a 53 ± 10 nm shell thickness when exposed to a power of 9 ± 1 W with a 2 minute continuous exposure.

In the case of experiments where a 10 minute exposure time was used, an increase of temperature was observed up to a maximum temperature of 59.3 °C. To confirm that capsule breakage was due to cavitation and not simply an effect of heating, each sample was also heated and maintained at 60 °C for 30 minutes. Figures S1a-d show clearly that prior to ultrasound application, the capsules are spherical with a fully intact shell for each shell thickness. For the samples heated to 60 °C (fig. S1e-h) the capsules at each shell thickness show none of the obvious signs of rupture compared to those seen after exposure to ultrasound. However there are signs of damage in the form of holes for the thicker shelled samples, or buckling on the thinner shells, visible on some of the capsules. In contrast, the four samples, which have been subjected to ultrasound (fig. S1i-l) all show clear signs of rupture (bursting).

Focused ultrasound for rupture of microcapsules

Focused ultrasound is used clinically as a non-invasive therapeutic technology capable of penetrating deep tissues in the body. The fundamental principles behind focused ultrasound allow for multiple beams of ultrasound to be concentrated onto one target, thus minimising damage to the surrounding tissues, where exposure is to a single ultrasound beam. Thus, for potential translation of metal microcapsules as a therapeutic drug delivery vehicle it is preferable to use focused ultrasound. Therefore, MRI-guided focused ultrasound was investigated as a trigger for rupture of the metal coated polymer microcapsules in vitro. Two samples of gold microcapsules, with shell thicknesses of 53 ± 10 nm and 80 ± 10 nm, respectively, were subjected to three different ultrasound pressures, 5 MPa, 2.5 MPa and 0.5 MPa, corresponding to a forward power of 14 W, 3.7 W and 0.16 W. Based on the results of the standard ultrasound experiments, it was expected that 14 W would cause capsule rupture and so this highest power was chosen to compare with the conditions explored in the previous section. However this high power is unsuitable for clinical applications due to excessive tissue heating and potential lesions and haemorrhage.[33] The SEM micrographs in Figure 2 clearly show that at all three powers, the thinner (53 nm) shelled gold microcapsules have ruptured when compared to the non-exposed microcapsules (Fig 2a), although it appears that at 14 W (5 MPa), the bursting force is much more intense as

these capsules are completely collapsed with clear evidence of an dramatic burst release (Fig 2b). At 3.7 W and 0.16 W the capsules show significant evidence of collapse, with jagged edges of broken capsules easily noticeable for a number of capsules (Fig 2c and d). This suggests that while the ultrasound is not as damaging for the gold shells at 0.16 W, the capsules do indeed break at this lower power. This may be advantageous when activating drug release in the body to avoid small metal shell fragments from separating from the main broken capsules.

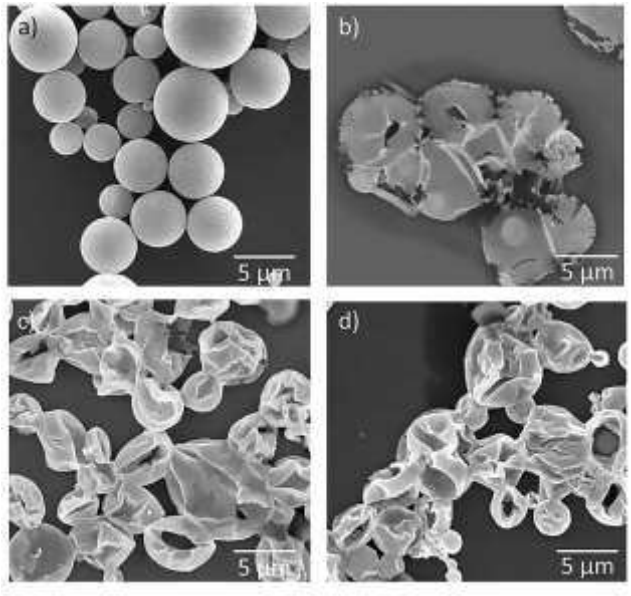

Figure 2 - Scanning electron micrographs showing gold coated polymer microcapsules with a shell thickness of 53 ± 10 nm a) pre-FUS and after FUS exposure of 10 ms bursts per second for 2 minutes at b) 14 W, c) 3.7 W and d) 0.16W.

For the thicker (~80 nm) gold shell microcapsules however, the majority of the capsules remain intact across the entire power range that was tested, revealing that the marginally thicker shells are able to better withstand the pressures imposed on them by the focused ultrasound (Figure 3). At 14 W the larger capsules show some signs of bursting in the form of holes appearing in their structure. However, most of these capsules remain spherical and intact. This damage differs to that caused by heating, seen in figure S2, as the increase in bulk temperature when using focused ultrasound is minimal.[34] At 3.7 W and 0.16 W the largest capsules show evidence of deformation in some cases, while a small number of the smaller capsules appear to show defects in their shells. This observation is in accordance with studies in the literature, which show that at powers below those that trigger immediate rupture, microcapsules show evidence of buckling or deformation.[21, 30] It is clear from these results using focused ultrasound that the capsule propensity to rupture upon application of ultrasound is highly dependent on the metal shell thickness. In addition, when considering capsules with thick metal shells, the size of the capsule appears to also affect the ultrasound response. Whilst this behaviour differs from the standard ultrasound results, it is important to note here that the focused ultrasound was delivered in 10 ms bursts every 1 s for the total exposure time of 2 minutes, as opposed to the continuous wave exposure used in the first part of this work. This FUS duty cycle was chosen to match dose regimes applied in a clinical setting.

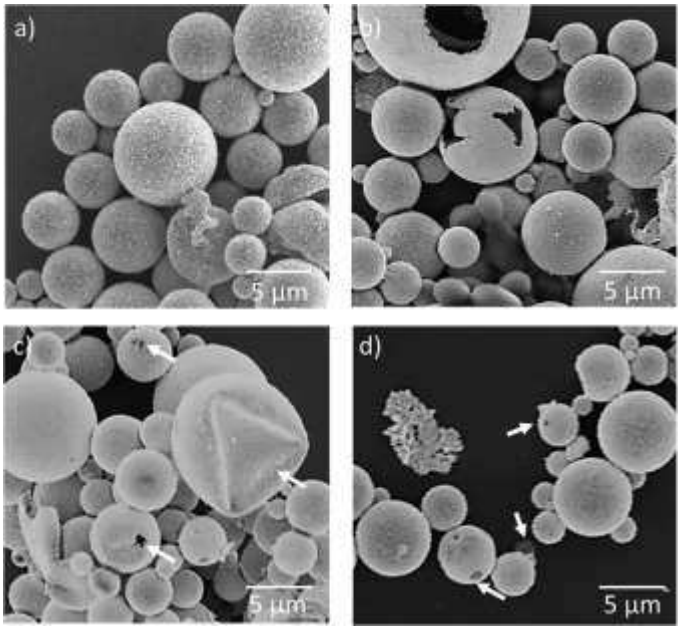

Figure 3 - Scanning electron micrographs showing gold coated polymer microcapsules with a shell thickness of 80 ± 10 nm a) pre-FUS and after FUS exposure of 10 ms bursts per second for 2 minutes at b) 14 W, c) 3.7 W and d) 0.16W. Arrows indicate damage to microcapsules caused by FUS.

3.4 Rupture of gold-shelled emulsions using FUS

In order to produce less structurally integral microcapsules and potentially improve the response to ultrasound, microcapsules consisting of an oil-core with a gold shell deposited directly at the oil-water interface (in the absence of an underlying polymer film) were synthesised. By removing the polymer film, we hypothesised that the capsules would lose some of their elastic properties,[31] thus becoming more brittle and easier to break. Two different gold shell thicknesses were used in this part of the work. The thinner shells were found to collapse on drying and so a higher concentration of gold salt was used in the electroless deposition reaction to obtain a second set of gold-coated emulsions of larger metal shell thickness, which remained intact after drying. The thinner shells were found to be approximately 80 nm, using AFM to measure a height profile across the collapsed capsule. The thickness of the gold-shelled emulsions which were able to retain their structure upon drying was obtained using our standard method of serial block face imaging of the sample embedded in resin. The resulting cross-sections were analysed using an in-house generated Matlab script, as described in our previous work,[17] and the thickness was found to be approximately 250 nm.

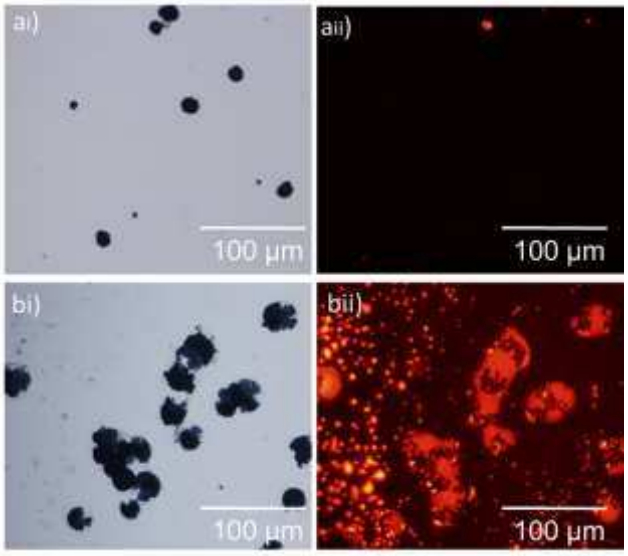

Figure 4 - Optical microscopy images of a_i gold coated emulsions in solution (bright field), a_{ii}) corresponding fluorescence microscopy image showing no signal from encapsulated DiI, a_{iii}), b_i) gold coated emulsions after mechanical fracture (bright field), b_{ii}) corresponding fluorescence microscopy image showing signal from released DiI

Optical microscopy images in Figure 4 show that intact gold shells block the fluorescence signal from the encapsulated dye DiI (Figure 4a_i and $_{ii}$), however once the shells are broken, the dye is released (Figure 4bi and ii), confirming that fluorescence emission from the dye has not been affected by the gold plating reaction. The fluorescence in Figure 4bii is evident in the liquid that has been released from the broken capsules.

3.5 FUS-triggered release of dye from gold-shell emulsions

A limitation of semi-quantitative method of calculating the proportion of ruptured capsules using observations of the resulting microcapsule structure from SEM is that the capsules could only be confidently separated into two categories: burst or intact. Capsules which appeared to have small defects such as cracks, of wrinkles were not treated as broken in the analysis. This potentially led to an underestimation of the damage due to ultrasound as such cracks and minor damage could allow for a slow release of the capsule contents. Thus, in this section, a fluorescent dye, DiI was encapsulated in the microcapsule core to allow for rupture of the capsules to be determined in terms of the dye release. To quantify release of the encapsulated dye from the gold-shell emulsions, FUS was applied to samples at 0.16 W, 3.7 W, and 14 W as in the previous section. The capsules were subjected to two different environments, aqueous solution and a hydrogel matrix. The hydrogel matrix, consisting of a 15 wt% solution of PLGA-PEG-PLGA in water, was chosen to represent the delivery of an active in an implantable drug delivery device, with drug-loaded microcapsules dispersed throughout the hydrogel. The hydrogel was designed to be thermo-setting, with a gelation temperature of 18 ℃, below which the polymer remained in solution. The capsule dispersion made up 10% by volume of the total gel or aqueous sample, with the capsules themselves occupying approximately 0.1% by volume of the sample.

After FUS exposure, the samples were refrigerated to allow the hydrogel to return to its liquid state, then ethanol was added to dissolve the polymer and create a 50:50 ethanol:water solvent to quantify release of DiI using fluorescence spectroscopy. Controls for microcapsules of each shell thickness that had not been exposed to FUS were also analysed for DiI release, and showed no release over 35 days (Figure 5b). Figure

5a shows the release of DiI from two gold-shell emulsion samples with different shell thicknesses, 35 days post ultrasound in either aqueous or hydrogel bulk phases. The results indicate that not all the capsules were broken. The capsules exposed to FUS in an aqueous environment released less dye than their counterparts in the hydrogel bulk solution, across all powers tested. This is potentially due to the restrictive forces holding the capsules in place within the hydrogel matrix making them more vulnerable to rupture by ultrasound, as opposed to in aqueous solution where the capsules are able to move freely, potentially dissipating the applied ultrasound force. The data in Figure 5a also suggest that, for all powers tested, the samples with thicker gold shells have released more dye than those with thinner shells, regardless of the bulk environment. This is most likely due to the thicker shells having less flexibility and so being unable to deform and buckle in response to the ultrasound waves, thus to dissipate the pressure they must rupture. Figure 5a also shows that whilst there is no significant difference in behaviour of the capsules at 0.16 W and 3.7 W (45-55 %), considerably less dye (20 %) is released from those capsules with thick shells in the hydrogel matrix at 14 W. One possible explanation for this observation is that, at this higher power, the hydrogel is damaged[35] and can no longer restrain the capsules, allowing them some freedom of movement which serves to dissipate the ultrasound power, thus avoiding rupture.

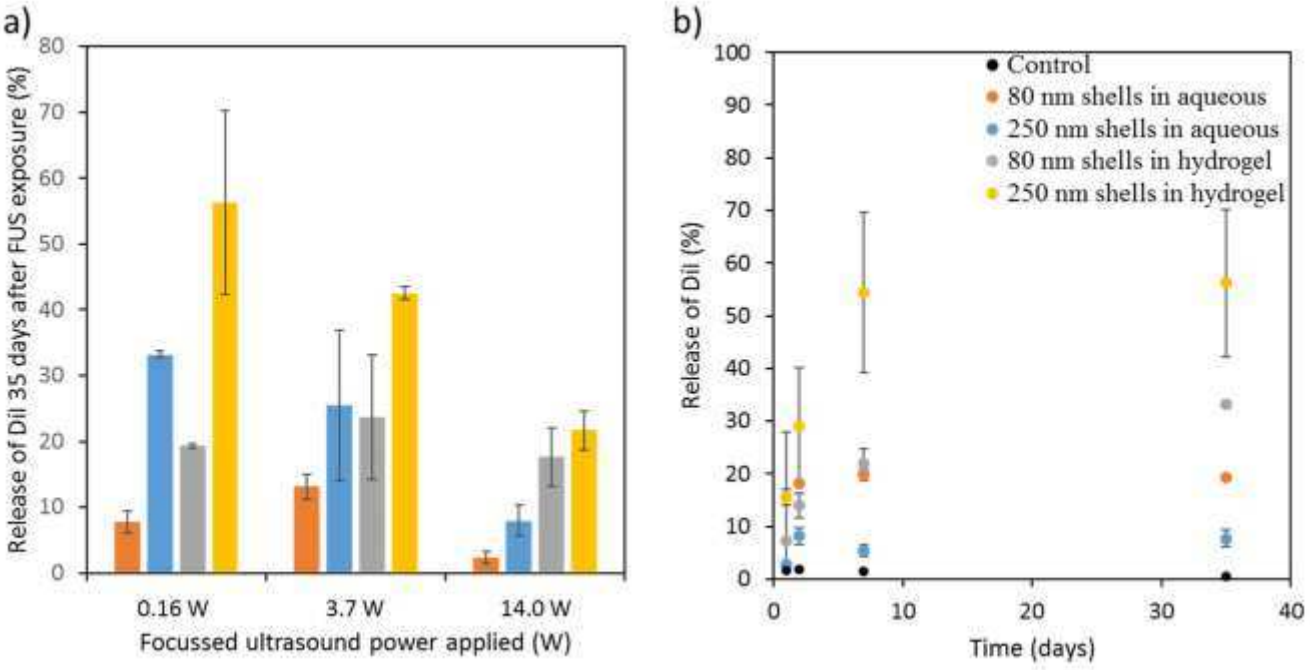

Figure 5 - Release of DiI a) as a function of FUS power applied (after 35 days) and b) over time, after FUS treatment, for 80 nm gold shell emulsion-templated microcapsules in aqueous suspension (orange), 250 nm gold shell emulsion-templated microcapsules in aqueous suspension (blue), 80 nm gold shell emulsion-templated microcapsules in hydrogel (grey) and 250 nm gold shell emulsion-templated microcapsules in hydrogel (yellow). Release from the control sample, which was not exposed to FUS is shown in black.

Figure 5b shows a sustained release from the microcapsules embedded in a hydrogel matrix with full release, from ruptured capsules, occurring between 7 and 35 days. This suggests that rupture of these capsules is likely different to the bursting seen for the metal-coated polymer shell microcapsules, suggesting the formation of cracks in the gold shells which, whilst allowing the dye to be released over time, are diffusion-limiting.

The emulsion-templated capsules did not have a smooth spherical appearance (Figure 6a), however, after exposure to FUS, the capsules have larger craters and wrinkles and appear to be more flaccid (Figure 6b). This supports the theory that small cracks may have formed during FUS exposure to allow for release of the dye as opposed to the burst rupture observed for the polymer shell gold microcapsules (Figure 2). The thinner, 80 nm, gold shelled emulsions collapsed upon drying, which prevented SEM to be used for efficient characterisation of these samples. However, reflected light optical microscopy conducted on the wet sample indicates a similar, uneven surface to that seen for the thicker shells (Figure 6c).

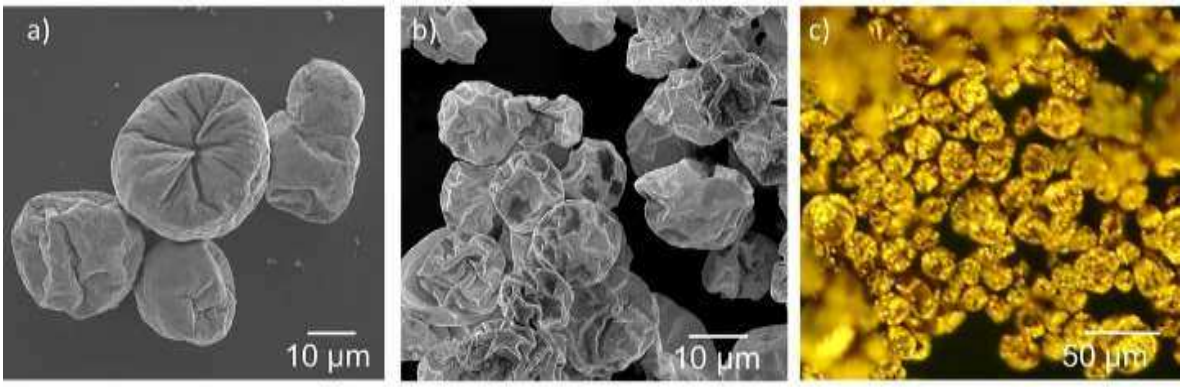

Figure 6 – a) Scanning electron micrograph of 250 nm gold shelled emulsion pre FUS and b) post FUS exposure at 0.16 W in a hydrogel bulk phase, c) optical microscopy image of 80 nm gold-shelled emulsion obtained using reflected light. Note that the 80 nm shells could not withstand drying and therefore could not be observed by SEM.

These findings confirm that FUS is suitable for use as an external trigger for sustained release from gold microcapsules embedded in a hydrogel matrix, suggesting that such systems could form suitable implantable devices for drug delivery.

Conclusions

The responsive nature of gold microcapsules with and without an intermediary polymer shell has been explored in this work. In order for impermeable gold microcapsules to be used as a drug delivery vehicle there is a requirement that an external stimulus can trigger the release of the encapsulated drug. Initial testing with a non-focused ultrasound transducer indicated that polymer microcapsules with a secondary gold shell could be ruptured across a range of ultrasound powers, in the order of literature values seen for metal nanoparticle decorated polymer microcapsules.[26] The percentage of microcapsules that ruptured was a function of the shell thickness. To apply the findings to clinical applications, a focused ultrasound was used as the external trigger to rupture the microcapsules. FUS successfully ruptured polymer-gold shell microcapsules at powers as low as 0.16 W and a shell thickness response dependence was observed. This is in line with clinically safe ultrasound powers, and requires a lower frequency and power of ultrasound than previously reported for metal coated microcapsules.[18] When the polymer shell was omitted from the capsule structure, it was discovered that in aqueous solution the capsules were less responsive to FUS, however when the capsules were embedded in a hydrogel matrix, release of the encapsulated dye was observed for both shell thicknesses, over a period of 28 days. This observation is critical to the progression of this technology as an effective clinical drug delivery device. This work confirms our hypothesis that FUS, at clinically acceptable powers, is an appropriate external trigger for the release of drug from inside gold

microcapsules embedded in a hydrogel carrier, allowing application as an implantable drug delivery device. Future work will investigate the encapsulation and release of a fluorescently labelled drug molecule to assess the feasibility of using metal shell microcapsules as an ultrasound- triggered, controlled release drug delivery vehicle.

Acknowledgements

The authors acknowledge the University of Queensland for the award of an Early Career Research Grant to ALW and funding from the CSIRO Probing Biosystems Future Science Platform enabling this work to be conducted. We also acknowledge the facilities, and the scientific and technical assistance, of the Australian Microscopy & Microanalysis Research Facility at the Centre for Microscopy and Microanalysis, The University of Queensland. This work was performed in part at the Queensland node of the Australian National Fabrication Facility (ANFF).

References

1. Yang, Z.; Peng, Z.; Li, J.; Li, S.; Kong, L.; Li, P.; Wang, Q., Food Chem **2014,** 145, 272-7.
2. Maswal, M.; Dar, A. A., Food Hydrocolloids **2014,** 37, 182-195.
3. Lee, H.; Choi, C. H.; Abbaspourrad, A.; Wesner, C.; Caggioni, M.; Zhu, T.; Weitz, D. A., ACS Appl Mater Interfaces **2016,** 8 (6), 4007-13.
4. Li, Y.; Huang, Y. Q.; Fan, H. F.; Xia, Q., Journal of Applied Polymer Science **2014,** 131 (7).
5. Tasker, A. L.; Hitchcock, J. P.; He, L.; Baxter, E. A.; Biggs, S.; Cayre, O. J., J Colloid Interface Sci **2016,** 484, 10-16.
6. Chaize, B.; Colletier, J. P.; Winterhalter, M.; Fournier, D., Artificial cells, blood substitutes, and immobilization biotechnology **2004,** 32 (1), 67-75.
7. Sun, C.; Shu, K.; Wang, W.; Ye, Z.; Liu, T.; Gao, Y.; Zheng, H.; He, G.; Yin, Y., Int J Pharm **2014,** 463 (1), 108-14.
8. Cui, J. W.; Wang, Y. J.; Postma, A.; Hao, J. C.; Hosta-Rigau, L.; Caruso, F., Advanced Functional Materials **2010,** 20 (10), 1625-1631.
9. Dowding, P. J.; Atkin, R.; Vincent, B.; Bouillot, P., Langmuir **2004,** 20 (26), 11374-9.
10. Feczko, T.; Kardos, A. F.; Nemeth, B.; Trif, L.; Gyenis, J., Polym. Bull. **2014,** 71 (12), 3289-3304.
11. Ito, F.; Kawakami, H., Colloids Surf. A **2015,** 482, 734-739.
12. Dowding, P. J.; Atkin, R.; Vincent, B.; Bouillot, P., Langmuir **2005,** 21 (12), 5278-84.
13. Hitchcock, J. P.; Tasker, A. L.; Baxter, E. A.; Biggs, S.; Cayre, O. J., ACS Appl Mater Interfaces **2015,** 7 (27), 14808-15.
14. Patchan, M. W.; Baird, L. M.; Rhim, Y. R.; LaBarre, E. D.; Maisano, A. J.; Deacon, R. M.; Xia, Z.; Benkoski, J. J., ACS Appl Mater Interfaces **2012,** 4 (5), 2406-12.
15. Sun, Q.; Routh, A. F., European Polymer Journal **2016,** 77, 155-163.
16. Tasker, A. L.; Hitchcock, J.; Baxter, E. A.; Cayre, D. O. J.; Biggs, S., Chemistry – An Asian Journal **2017,** 12 (13), 1641-1648.
17. Tasker, A. L.; Puttick, S.; Hitchcock, J.; Cayre, O. J.; Blakey, I.; Whittaker, A. K.; Biggs, S., J. Mater Chem. B **2018,** 6 (14), 2151-2158.
18. Sun, Q.; Gao, H.; Sukhorukov, G. B.; Routh, A. F., ACS Applied Materials & Interfaces **2017,** 9 (38), 32599-32606.
19. Huang, J. X.; Li, W. B.; Li, Y.; Luo, C. D.; Zeng, Y. C.; Xu, Y. H.; Zhou, J. H., J. Mater Chem. B **2014,** 2 (39), 6848-6854.
20. Kooiman, K.; Bohmer, M. R.; Emmer, M.; Vos, H. J.; Chlon, C.; Shi, W. T.; Hall, C. S.; de Winter, S. H.; Schroen, K.; Versluis, M.; de Jong, N.; van Wamel, A., Journal of controlled release : official journal of the Controlled Release Society **2009,** 133 (2), 109-18.
21. Lensen, D.; Gelderblom, E. C.; Vriezema, D. M.; Marmottant, P.; Verdonschot, N.; Versluis, M.; de Jong, N.; van Hest, J. C. M., Soft Matter **2011,** 7 (11), 5417-5422.
22. Wang, C. Y.; Yang, C. H.; Lin, Y. S.; Chen, C. H.; Huang, K. S., Biomaterials **2012,** 33 (5), 1547-53.

23. Wang, X.; Chen, H.; Zhang, K.; Ma, M.; Li, F.; Zeng, D.; Zheng, S.; Chen, Y.; Jiang, L.; Xu, H.; Shi, J., Small **2014,** 10 (7), 1403-11.
24. Antipina, M. N.; Sukhorukov, G. B., Adv Drug Deliv Rev **2011,** 63 (9), 716-29.
25. Skirtach, A. G.; De Geest, B. G.; Mamedov, A.; Antipov, A. A.; Kotov, N. A.; Sukhorukov, G. B., J. Mater Chem **2007,** 17 (11), 1050-1054.
26. Kijewska, K.; Glowala, P.; Wiktorska, K.; Pisarek, M.; Stolarski, J.; Kepinska, D.; Gniadek, M.; Mazur, M., Polymer **2012,** 53 (23), 5320-5329.
27. Qiao, M.; Chen, D.; Ma, X.; Liu, Y., Int J Pharm **2005,** 294 (1-2), 103-12.
28. Schneider, C. A.; Rasband, W. S.; Eliceiri, K. W., Nat Methods **2012,** 9 (7), 671-5.
29. Stark, K.; Hitchcock, J. P.; Fiaz, A.; White, A. L.; Baxter, E.; Biggs, S. R.; McLaughlan, J.; Freear, S.; Cayre, O. J., ACS Applied Materials & Interfaces **2019**.
30. Marmottant, P.; Bouakaz, A.; Jong, N. d.; Quilliet, C., The Journal of the Acoustical Society of America **2011,** 129 (3), 1231-1239.
31. Pavlov, A. M.; Saez, V.; Cobley, A.; Graves, J.; Sukhorukov, G. B.; Mason, T. J., Soft Matter **2011,** 7 (9), 4341-4347.
32. Kolesnikova, T. A.; Khlebtsov, B. N.; Shchukin, D. G.; Gorin, D. A., Nanotechnologies in Russia **2008,** 3 (9), 560-569.
33. Hynynen, K.; Vykhodtseva, N. I.; Chung, A. H.; Sorrentino, V.; Colucci, V.; Jolesz, F. A., Radiology **1997,** 204 (1), 247-253.
34. Ebbini, E. S.; Ter Haar, G., International Journal of Hyperthermia **2015,** 31 (2), 77-89.
35. Movahed, P.; Kreider, W.; Maxwell, A. D.; Hutchens, S. B.; Freund, J. B., The Journal of the Acoustical Society of America **2016,** 140 (2), 1374-1374.